JGR Earth Surface

RESEARCH ARTICLE
10.1029/2023JF007148

Rethinking Variability in Bedrock Rivers: Sensitivity of Hillslope Sediment Supply to Precipitation Events Modulates Bedrock Incision During Floods

Clarke DeLisle[1] **and Brian J. Yanites**[1]

[1]Department of Earth and Atmospheric Sciences, Indiana University Bloomington, Bloomington, IN, USA

Key Points:

- We present a bedrock river evolution model that accounts for sediment supply sensitivity to precipitation events over long timescales
- When sediment supply is highly sensitive to large precipitation events, bedrock incision is inhibited by sediment cover during floods
- We find evidence of an upper limit on water discharge for river incision driven by increased sediment cover in channels

Supporting Information:

Supporting Information may be found in the online version of this article.

Correspondence to:

C. DeLisle,
cdelisle@iu.edu

Citation:

DeLisle, C., & Yanites, B. J. (2023). Rethinking variability in bedrock rivers: Sensitivity of hillslope sediment supply to precipitation events modulates bedrock incision during floods. *Journal of Geophysical Research: Earth Surface*, *128*, e2023JF007148. https://doi.org/10.1029/2023JF007148

Received 3 MAR 2023
Accepted 23 AUG 2023

Abstract Bedrock rivers are the pacesetters of landscape evolution in uplifting fluvial landscapes. Water discharge variability and sediment transport are important factors influencing bedrock river processes. However, little work has focused on the sensitivity of hillslope sediment supply to precipitation events and its implications on river evolution in tectonically active landscapes. We model the temporal variability of water discharge and the sensitivity of sediment supply to precipitation events as rivers evolve to equilibrium over 10^6 model years. We explore how coupling sediment supply sensitivity with discharge variability influences rates and timing of river incision across climate regimes. We find that sediment supply sensitivity strongly impacts which water discharge events are the most important in driving river incision and modulates channel morphology. High sediment supply sensitivity focuses sediment delivery into the largest river discharge events, decreasing rates of bedrock incision during floods by orders of magnitude as rivers are inundated with new sediment that buries bedrock. The results show that the use of river incision models in which incision rates increase monotonically with increasing river discharge may not accurately capture bedrock river dynamics in all landscapes, particularly in steep landslide prone landscapes. From our modeling results, we hypothesize the presence of an upper discharge threshold for river incision at which storms transition from being incisional to depositional. Our work illustrates that sediment supply sensitivity must be accounted for to predict river evolution in dynamic landscapes. Our results have important implications for interpreting and predicting climatic and tectonic controls on landscape morphology and evolution.

Plain Language Summary Rivers that carve rock are often used as markers of climate, tectonic, and rock-type controls in evolving landscapes. To back out these controls from the present form of rivers which erode rock, thorough knowledge of how they evolve and how they respond to changes in climate and tectonics is required. Most models for the evolution of bedrock rivers assume that the rate of erosion always increases with river discharge, as the weight of water on the riverbed increases. Here, we challenge this assumption using a new model for river evolution which accounts for short-timescale variations in river discharge and supply of sediment from hillslopes to channels. We find that in these systems, the largest floods may be less erosive than one would expect because they must transport large volumes of sediment, which makes it harder for them to erode fresh bedrock in channels. Our results are important because models of river evolution inform much of our understanding of interactions between Earth's surface and its atmosphere in rapidly changing parts of our planet.

1. Introduction

In actively uplifting non-glaciated landscapes, bedrock rivers are the primary interface between atmospheric and solid Earth processes. These rivers adjust their slope, width, incision rates, and sediment transport capacities in response to a range of climatic and tectonic forcings, pacing landscape evolution and setting local baselevel to which surrounding hillslopes adjust their form. Understanding and building tools to predict bedrock river response to tectonics and climate is thus of paramount importance to quantitative geomorphology. Even so, studies reach disparate conclusions on how factors such as climate, tectonics, river discharge variability, rock type, and sediment supply impact the evolution of fluvial systems and the surrounding landscapes (Chen et al., 2019; Lague, 2014; Seybold et al., 2021; Yanites & Tucker, 2010). Previous work shows that the amount of water flowing through a river channel, and the temporal variability of this value, strongly influences bedrock river incision (Deal et al., 2017; DiBiase & Whipple, 2011; Ferrier et al., 2013; Forte et al., 2022; Lague et al., 2005; Molnar et al., 2006; Snyder et al., 2003). Likewise, sediment flux in a river channel is understood to influence

bedrock river incision and channel geometry (Cowie et al., 2008; Johnson et al., 2009; Lamb et al., 2008; Pfeiffer et al., 2017; Sklar & Dietrich, 2001, 2004). However, unlike water discharge variability, the influence of time varying sediment supply, and the sensitivity of that sediment supply to precipitation events, on the evolution of bedrock rivers and landscape evolution has seen relatively little attention (Campforts et al., 2022; Lague, 2010).

The most common approach to modeling evolving mountain rivers is the stream-power incision model (SPIM). The SPIM focuses on the dynamics of bedrock detachment, and generally explicitly or implicitly assumes that rivers are in a detachment limited state (Bull, 1979; Lague, 2014; Whipple & Tucker, 1999). The SPIM often uses contributing drainage area as a proxy for river discharge and assumes that bedrock incision rate increases monotonically with increasing discharge and channel slope. Countless studies have fit stream power models to specific study areas (Duvall et al., 2004; Kirby & Whipple, 2001, 2012; Perron & Royden, 2013; Snyder et al., 2000), while many have found the SPIM too simple to explain relationships between river morphology and incision rate (Forte et al., 2022; Scherler et al., 2017).

A first-order limitation of the SPIM is the assumption that river discharge is adequately represented using a long-term mean value. The recognition that bedrock river incision is a threshold process in which no geomorphic work is accomplished below a threshold for incision has led some to question the applicability of the original SPIM in rivers with significant incision thresholds (Lague, 2014; Lague et al., 2005; Tucker, 2004). To overcome this limitation, a version of the SPIM was proposed using a threshold shear stress for river incision. This threshold is commonly assumed to represent the shear stress required for the initiation of sediment motion, though it could also be set by thresholds for erosional processes such as plucking.

The presence of a threshold for bedrock river incision highlights the importance of considering the distributions of river discharge when modeling bedrock rivers. In a threshold incision framework, small discharge events accomplish no geomorphic work while large, rare events play an outsized role in river and landscape evolution. Lague et al. (2005) recognized the importance of this behavior and documented relationships between the return time of erosive storms and channel slope. Molnar et al., 2006 used data from 440 river gauges in the United States and found a positive relationship between river discharge variability and bedrock incision rates. DiBiase and Whipple (2011) calibrated a stochastic SPIM to data from the San Gabriel Mountains, concluding that given a significant threshold for bedrock incision, the distribution of water discharge events is a primary control on river evolution and equilibrium form. Other work suggests the importance of other factors which influence discharge variability, including snowmelt (Forte et al., 2022), gaining/losing hydrology (Chen et al., 2019), and ecohydrology (Rossi et al., 2016). These previous analyses point to the importance of discharge variability in evolving mountain rivers across a range of environments and suggest that rivers with more variable discharge are more erosive, all else being equal.

Despite intense focus by the geomorphic community on the importance of river discharge distributions to bedrock incision, far less work has been devoted to sediment supply, which also varies in time, and the sensitivity of that sediment supply to precipitation events. Here, we refer to this relationship as sediment supply sensitivity. Sediment plays a dual role in bedrock river evolution; it provides the tools which break and detach bedrock as they move downstream, but when sediment is deposited in a river channel, it covers bedrock and inhibits incision (Sklar & Dietrich, 2001). Processes of sediment delivery to bedrock rivers from surrounding hillslopes range from diffusive (e.g., soil creep, rain splash, freeze-thaw cycles) which are relatively steady in time to highly stochastic mass wasting (e.g., landslides and debris flows). This time-variable sediment supply impacts spatio-temporal patterns of sediment cover in bedrock rivers, which in turn affects the ability of a river to weather and erode bedrock (Yanites et al., 2011). An exceedingly small body of work (e.g., Lague, 2010) exists examining the impacts of time-variable sediment supply and cover on bedrock river evolution, but suggests that time-variable sediment supply is critical in understanding the coupled hillslope-fluvial system (Campforts et al., 2020, 2022). Previous investigation into these processes suggests that rivers can be classified as either "flood-depositing" or "flood cleaning" (Turowski et al., 2013), behaviors which are intimately linked to temporal processes of sediment delivery from hillslopes to channels. Our modeling framework explores the impact of sediment supply sensitivity on channel morphology and temporal patterns in bedrock river incision. We leverage the model to explore relationships between the magnitude of precipitation event and volume of sediment supplied from hillslopes to channels.

The sensitivity of sediment transport from hillslopes to channels to precipitation event magnitude is challenging to quantify. Sediment cover in bedrock eroding rivers is observed to change rapidly (Figure 1). Marc

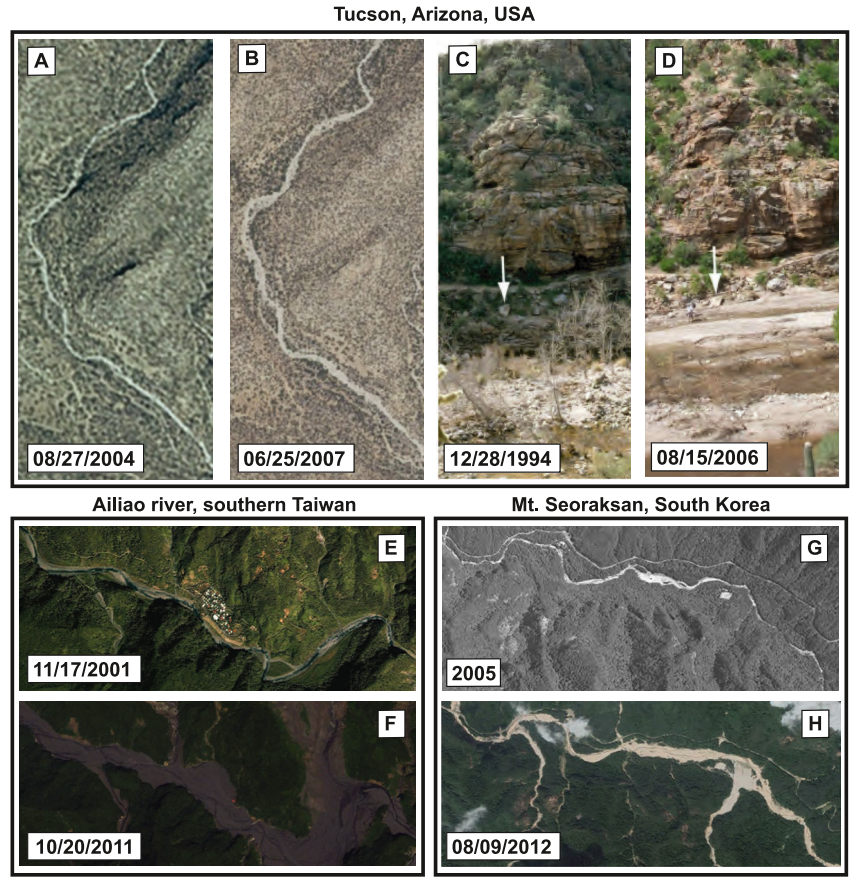

Figure 1. Evidence for rapidly changing sediment cover in incising rivers. (a–d) Changing sediment cover in the Santa Catalina mountains northeast of Tucson, AZ following heavy rainfall in the summer of 2006 (photos c and d from Webb et al., 2008). (e–f) Channel aggradation following landslides triggered by the 2009 typhoon Morakot in southern Taiwan (DeLisle et al., 2021; Marc et al., 2018). (g, h) Channel aggradation following a heavy summer rain in 2006 at Mt. Seoraksan, South Korea (Kim et al., 2021). All other photos from Google Earth.

et al. (2018) document the relationship between the largest river discharge events and the large sediment supply events that coincide with them, suggesting that large sediment supply events can occur during rare storms. Furthermore, diffusive processes of sediment supply (e.g., rain splash) can depend on precipitation intensity. Here we revisit existing understanding of river discharge variability and bedrock river evolution by explicitly accounting for sediment supply sensitivity in addition to stochastic river discharge on bedrock river incision.

We examine the combined impact of water discharge and sediment supply sensitivity by building on a recent 1D numerical model for river evolution (Yanites, 2018). We simulate stochastic water discharge in an evolving channel over geomorphic time in which sediment supply is linked to stochastic runoff events using a tunable power-law relationship. We interrogate our model for impacts of time-varying sediment supply on patterns of river incision, sediment cover dynamics, channel morphology, and partitioning of geomorphic work across the distribution of water discharge events. In existing frameworks for river evolution by stochastic bedrock incision, large and rare floods play an important role in bedrock incision and landscape evolution. Our model suggests that when sediment supply sensitivity is accounted for, this is not always the case. The ability of the largest floods to incise bedrock is impeded by the concurrent delivery of large volumes of sediment, decreasing peak single-event incision rates. Our modeling supports the hypothesis that, in some landscapes, most of the geomorphic work and bedrock incision occurs during events closer to the middle of the river discharge distribution where rivers have the power to overcome incision thresholds but are not buried by newly delivered sediment. Our work has implications for tectonic geomorphology and landscape evolution, improves our ability to use river profile analysis to quantify local tectonics, and impacts the search for evidence of climatically modulated tectonics.

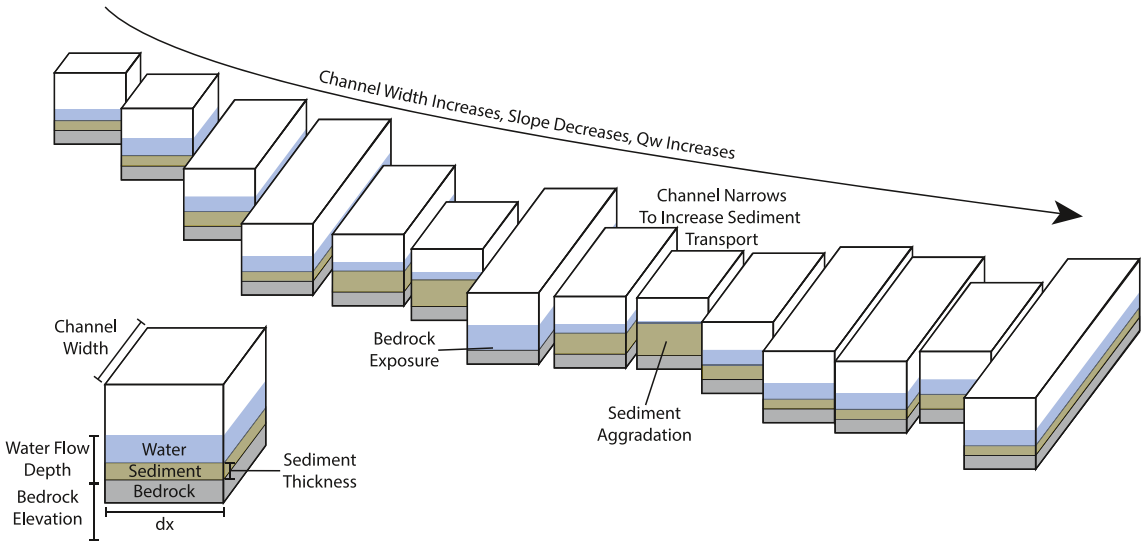

Figure 2. Model schematic. Each box represents one model node. At each node, the model uses modeled water discharge to approximate flow depth and boundary shear stress. The model has sediment input at each node and moves sediment downstream between nodes as a function of water discharge, channel width, grain size, and bed slope. Channel width evolves according to an optimization algorithm (Yanites, 2018). Bedrock elevation changes following the combined impact of rock uplift and bedrock erosion, and sediment thickness is determined by the competition of sediment supply and transport.

2. The Model

2.1. Model Overview

This modeling framework is a continuation of the work presented in Yanites (2018), modified to incorporate stochastic water discharge and sediment supply. The 1-D model accounts for constant rock uplift, which adds potential energy to the system by elevating the river channel above an unchanging reference elevation. Bedrock elevation evolves at a node in the model as the competition of this continuous rock uplift with bedrock erosion and sediment transport. Water discharge in the channel is drawn randomly from a distribution of values at each time step (dt = 1/24 yr), and sediment influx to the channel varies in time as a power-law function of water discharge. Our model is unique in that it allows us to investigate the impacts of sediment supply sensitivity in addition to stochastic water discharge over landscape evolution timescales. The model is schematically represented in Figure 2.

2.2. Evolution of Channel Elevation

In our model river, elevation of the channel (z_{channel}) includes the elevation of the bedrock channel (z_{bedrock}) and the thickness of sediment cover (h). Through time (t), z_{channel} is modified by rock uplift rate (U_{r}), bedrock incision I, and changes in h. When significant sediment cover exists, bedrock erosion is assumed to be zero due to bed shielding effects (Sklar & Dietrich, 2004). The change in z_{channel} is written as follows.

$$\frac{\partial z_{\text{channel}}}{\partial t} = \begin{cases} U_r - E & \text{when } h = 0 \\ U_r + \frac{\partial h}{\partial t} & \text{when } h > 0 \end{cases} \quad (1)$$

We allow the model to evolve through time until $\frac{\partial z_{\text{channel}}}{\partial t}$ approaches zero when averaged over 10^3 years, at which point the model reaches dynamic equilibrium. The stochastic nature of the model means that the channel never reaches a true equilibrium elevation where $\frac{\partial z_{\text{channel}}}{\partial t} = 0$, as z_{channel} is impacted by erosion and deposition even at dynamic equilibrium.

2.3. Bedrock Erosion

We model the erosion of bedrock using a modified stream power law that accounts for the presence or absence of immobile sediment protecting bedrock from detachment processes.

$$E = FK\tau_b^a \tag{2}$$

where K is rock erodibility, a is a constant equal to 1 (Whipple et al., 2000), and τ_b is basal shear stress. F is fractional bedrock exposure between zero (channel fully covered by sediment) and one (no sediment cover present the in channel). F varies as a ratio of sediment supply (Q_s) and sediment transport capacity (Q_t):

$$F = 1 - \frac{Q_s}{Q_t} \tag{3}$$

Sediment cover at each node in our model is the product of sediment transport downstream from node to node, as well as input to the channel from the hillslopes at each timestep. We show our handling of downstream sediment transport in Equation 8. Equation 2 is the incision law used in all models described here, but we note that the modeling framework readily extends to other incision rules (Yanites, 2018).

The boundary shear stress (τ_b, Equation 2) on the channel bed is

$$\tau_b = \rho g R S \tag{4}$$

where ρ is the density of water, g is gravitational acceleration, R is hydraulic radius, and S is channel slope. We assume a rectangular channel, thus

$$R = \frac{A_c}{P} = \frac{W H_{flow}}{W + 2H_{flow}} \tag{5}$$

where A_c is the cross-sectional area of flow in the channel, P is the wetted perimeter, W is channel width, and H_{flow} is flow depth. The rectangular channel assumption simplifies the modeling approach by allowing us to ignore at-a-station hydraulic geometry fluctuations with varying discharge (Leopold & Maddock, 1953) Flow depth is calculated using conservation of water discharge (Q_w) as follows:

$$Q_w = V A_c \tag{6}$$

using flow velocity (V) from Manning's equation.

$$V = \frac{1}{n} R^{2/3} S^{1/2} \tag{7}$$

where n is a Manning's roughness coefficient, which we set to 0.04. We solve the above system of equations (Equations 5–7) and estimate flow depth, H_{flow}. At each time step, Q_w is drawn from a distribution described below and used to estimate H_{flow} and τ_b.

2.4. Sediment Transport

We model bedload the evolution of sediment cover at each timestep in our model using the Exner equation (Exner, 1920, 1925; Paola & Voller, 2005):

$$\frac{\partial h}{\partial t} = -\frac{1}{(1-\lambda_p)} \frac{\partial q_s}{\partial x} \tag{8}$$

where q_s is sediment supply transported through a node per unit width, λ_p is the porosity of bedload sediment (constant at 0.2 for all model runs), and x is distance downstream.

Sediment transport capacity Q_t is calculated following a modified Meyer-Peter and Mueller equation (Meyer-Peter & Müller, 1948; Wong & Parker, 2006) as follows:

$$Q_t = 3.97 \rho_s W \left[\frac{\tau_b}{(\rho_s - \rho) g D} - \tau_c^* \right]^{1.5} D^{1.5} \sqrt{\frac{\rho_s - \rho}{\rho} g} \tag{9}$$

Where ρ_s is the density of sediment grains (2,650 kg/m^3) and τ_c^* is the Shields criterion assumed to be 0.045 (Wong & Parker, 2006). D is the grain size in the channel which fines downstream as a function of Sternberg's law (Sternberg, 1875):

$$D = D_o e^{-a_s x} \tag{10}$$

where D_o is the initial grain size at the river headwaters (constant across all model runs at 15 cm), x is distance downstream from channel head, and a_s is a downstream fining parameter.

2.5. Water Discharge

We use a modified inverse gamma distribution of nondimensional river discharge $Q_w{}^*$ which is commonly applied in studies on the impact of river discharge variability on river and landscape evolution (Crave & Davy, 2001; DiBiase & Whipple, 2011; Lague, 2010; Lague et al., 2005). The continuous probability distribution of nondimensional daily discharge events is as follows:

$$\mathrm{PDF}_{\overline{Q}w,k_v}(Q_w{}^*) = \frac{k_v{}^{k_v+1}}{\Gamma(k_v+1)}\exp\left(-\frac{k_v}{Q_w{}^*}\right)Q_w{}^{*-(2+k_v)}dQ_w{}^* \tag{11}$$

Where $Q_w{}^*$ is nondimensional mean daily discharge, and k_v controls discharge variability. Discharge variability is *higher* for *lower* values of k_v. Nondimensional discharge $Q_w{}^*$ is defined as

$$Q_w{}^* = \frac{Q_w}{\overline{Q_w}} \tag{12}$$

Where Q_w is actual water discharge and $\overline{Q_w}$ is mean daily discharge, a function of drainage area and mean daily runoff.

2.6. Sediment Supply

We develop a new approach to relate hillslope sediment supply to stochastic weather events. Our approach reflects the transfer of sediment from hillslopes to adjacent channels, not sediment supply variability due to waves of sediment moving through a channel network. We use a power-law relationship between nondimensional river discharge $Q_w{}^*$ and nondimensional sediment supply $Q_s{}^*$. The relationship is defined as follows:

$$Q_s{}^* = NQw^{*\eta} \tag{13}$$

where η is the sediment sensitivity exponent, which we vary to reflect differences in landscape response to weather events, $Q_s{}^*$ is nondimensional sediment supply to the channel from hillslopes, and N is a normalization parameter to set long-term mean sediment supply constant across model runs. $Q_s{}^*$ is defined as:

$$Q_s{}^* = {}^{Q_s}/_{\overline{Q_s}} \tag{14}$$

where $\overline{Q_s}$ is long-term average sediment supply,

$$\overline{Q_s} = \partial A(x)U_r \tag{15}$$

$\partial A(x)$ is the difference between contributing area at a node and the node upstream, and U_r is rock uplift rate. This approach sets long-term sediment supply as the total available rock volume entering the landscape through tectonic uplift, equal to contributing drainage area multiplied by rock uplift rate.

In Equation 13, N is a normalization coefficient which sets the mean value of $Q_s{}^*$ equal to one even as the value of η is changed, setting long term mean sediment delivery equal to $\overline{Q_s}$. N is defined as

$$N = \left[\langle PDF_{\underline{Q},k}(Qw^*)\rangle_{Qw^*\eta}\right]^{-1} \tag{16}$$

where the denominator in Equation 16 is the expectation value of Equation 11 evaluated at $Ow^{*\eta}$. This approach allows us to vary η to test different degrees of sediment variability while keeping long-term volumes of sediment supply constant across model runs.

At each timestep, sediment supply is delivered to each node using the same value of $Q_s{}^*$, with absolute values of sediment input being a function of $Q_w{}^*$, contributing drainage area, and rock uplift rate. Our model does not account for spatial heterogeneity of sediment input along the channel profile.

When η is equal to one, sediment delivery varies linearly with water discharge such that larger storms deliver proportionally more sediment. For values of η less than one, sediment delivery is less than proportional to water

discharge, where large storms increase sediment delivery at a rate slower than the rate of increase in water discharge. For values of η greater than one, large storms play an outsized role in sediment delivery and sediment supply is concentrated into large, rare events. We apply this scheme to represent differences in sediment delivery dictated by hillslope sediment transport mechanics.

Sediment supply in this model is tied directly to non-dimensional river discharge Q_w^*. For a model run with a constant value of η, Q_s^* will always be the same for a given value of Q_w^*. Our model does not account for factors which may change sediment supply sensitivity to precipitation events (e.g., wildfires or earthquakes). The modeling framework could be extended to incorporate these effects by varying the parameter η in space and/or time, but we do not believe that the omission of these effects detracts from the results presented here. Our model does not account for required recharge time for hillslope sediment supply between successive large events due to processes of rock weathering and soil production. Repeated rare events will drive the same volume of sediment supply regardless of the time between events. Again, time variable η values in a future study could account for such factors.

2.7. Model Parameterization

The equations in Section 2.3 show the importance of channel width in controlling basal shear stress, which drives bedrock incision and sediment transport. As such, we avoid using prescribed and fixed channel widths. Instead, we optimize channel width to maximize bedrock incision and sediment transport. We use the channel width optimization algorithm of Yanites (2018) to incorporate evolving channel width in response to tectonic, hydrologic, and sediment supply forcings. This heuristic approach to channel width simplifies channel width calculation and reproduces expected width responses to changes in rock uplift, discharge, and sediment supply (Yanites, 2018). At each time step, the model calculates channel width at each node and determines if maintaining, increasing, or decreasing width relative to the previous timestep will maximize bedrock incision (or sediment transport in times of complete sediment cover) with the current water discharge and channel slope. The model does this by solving the necessary equations to estimate E (Equation 2) or Q_t (Equation 9) under three different channel width scenarios (constant width, wider, or narrower) and evolving to maximize geomorphic work.

The degree to which a channel can widen or narrow at a given time and location depends on the boundary shear stress in the channel at the time:

$$W = W_i \pm k_w \tau_b \tag{17}$$

where W_i is channel width at the node at the previous timestep, and k_w is a channel width adjustment constant. We use $k_w = 0.01$ for all models presented here. The physical parameters which control k_w include lithology, bank material, vegetation, climate, and many others. We chose a value of k_w such that changes in channel width are small (<10% of channel width) after model spin-up (see Supporting Information S1).

Many of the general controlling parameters for this model (e.g., starting channel width, mean water discharge, drainage area, bedload sediment size) are functions of distance downstream from the channel head. These variables are held constant across model runs presented here. We chose values for these parameters which yield physically reasonable water discharges (ranging from near zero to >200 m^3/s), grain sizes (ranging from >10 cm in headwaters to <1 cm at the channel mouth), and drainage areas (~2,000 km^2); we have not calibrated these variables to represent a single specific river or landscape.

We define a 100 km river reach divided into 50 nodes with 2 km node spacing. Mean river discharge at each node scales directly with drainage area (A) as follows:

$$\overline{Q_w} = k_Q A^c \tag{18}$$

We set the exponent c to 1, thus k_Q is an upstream runoff term. Drainage area is estimated using Hack's law (Hack, 1957):

$$A = C_h x^{H_e} \tag{19}$$

where C_h (equal to 1) and H_e (equal to 1.8598) are empirical constants. We provide the model with an initial channel width, W_o as a function of $\overline{Q_w}$:

$$W_o = k_{wa} \overline{Q_w}^b \tag{20}$$

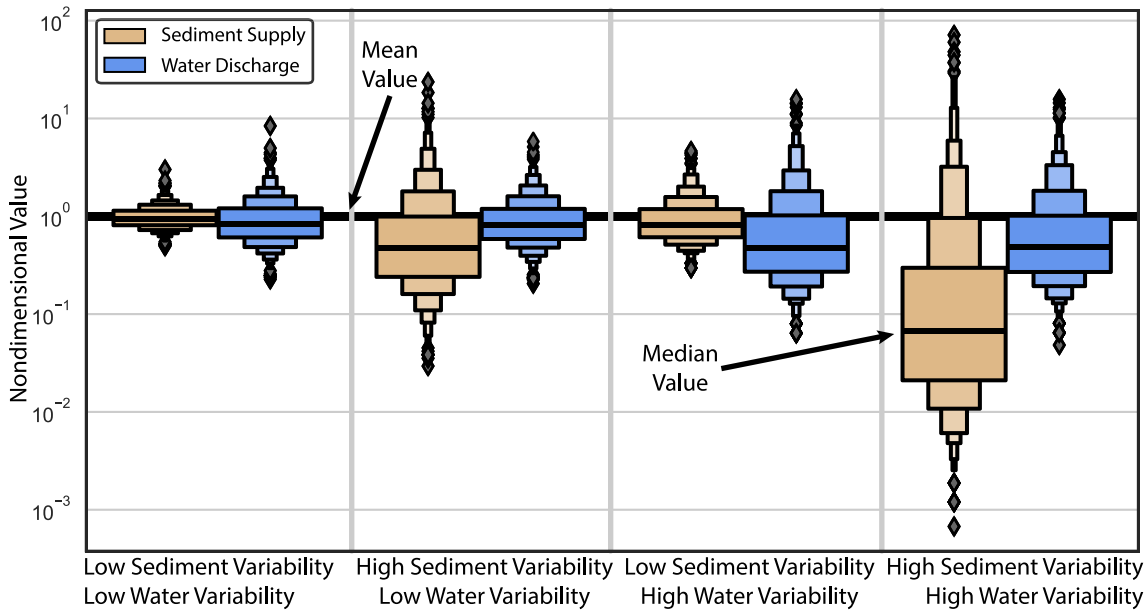

Figure 3. Boxen plot showing nondimensional values of water discharge and sediment supply as defined in Equations 11 and 13. Changes in box width represent percentiles, and are comparable across the figure. Distributions are defined by drawing 1,000 random samples of $Q_w{}^*$ from Equation 11 and using those values in Equation 13 to calculate values of $Q_s{}^*$. Low water discharge variability scenarios use $k_v = 3.0$ and high-water variability scenarios use $k_v = 0.3$; low sediment variability scenarios use $\eta = 0.5$ and high sediment variability scenarios use $\eta = 2.0$.

where k_{wq} (equal to 5) and b (equal to 0.3) are empirical constants.

2.8. Numerical Experiments

The primary goal of this study is to assess the combined role of and the tradeoffs between water discharge variability (k_v, Equation 11), and sediment supply sensitivity (η, Equation 13) in governing river morphology and patterns of river incision in equilibrium channels. Our model is unique in its consideration of these two variables in tandem, and in that it is computationally efficient enough to compute sediment transport and channel width changes over long timescales with stochastic river discharge and time-varying sediment supply. We present a suite of model runs in which we covary k_v and η to represent a range of possible behaviors of real-world landscapes.

We vary water discharge variability (k_v) in Equation 11 from 0.3 (high variability river systems such as the arid American southwest or the typhoon-dominated Taiwan orogen) to 3.0 (low variability rivers such as those of the American Midwest) (Crave & Davy, 2001; DiBiase & Whipple, 2011). In our model framework high water discharge variability rivers are ones which are generally in a state of low flow but are punctuated by rare large floods. Low discharge variability rivers are ones which have variations in their discharge but are generally near their mean flow. We ensure across all models that long term mean river discharge ($\overline{Q_w}$) is held constant, a function only of Equation 11.

To control sediment supply sensitivity, we vary η in Equation 13 between 0.25 and 2.0. Low values of η keep $Q_s{}^*$ closer to $\overline{Q_s}$ through time; higher values of η increase the importance of large, rare sediment supply events which are tied to large floods. The normalization factor N in Equation 13 keeps $\overline{Q_s}$ consistent across model runs. $\overline{Q_s}$ varies according to the prescribed rock uplift rate, where models with higher rock uplift rates have higher $\overline{Q_s}$.

Figure 3 shows endmember regimes of water discharge and sediment supply sensitivity to a node near the headwaters of the model domain. Distributions of sediment supply events are longer tailed when sediment variability is high ($\eta = 2.0$) than when sediment variability is low ($\eta = 0.25$). Following Equation 13, sediment supply is more variable when water discharge variability is higher, even when η is the same. This is illustrated in Figure 3 by comparing sediment supply distributions for the low water discharge variability—low sediment variability example with the high water discharge variability—low sediment variability example. The tails on the distribution of sediment supply events are longer when water discharge variability is high, even when η is held constant.

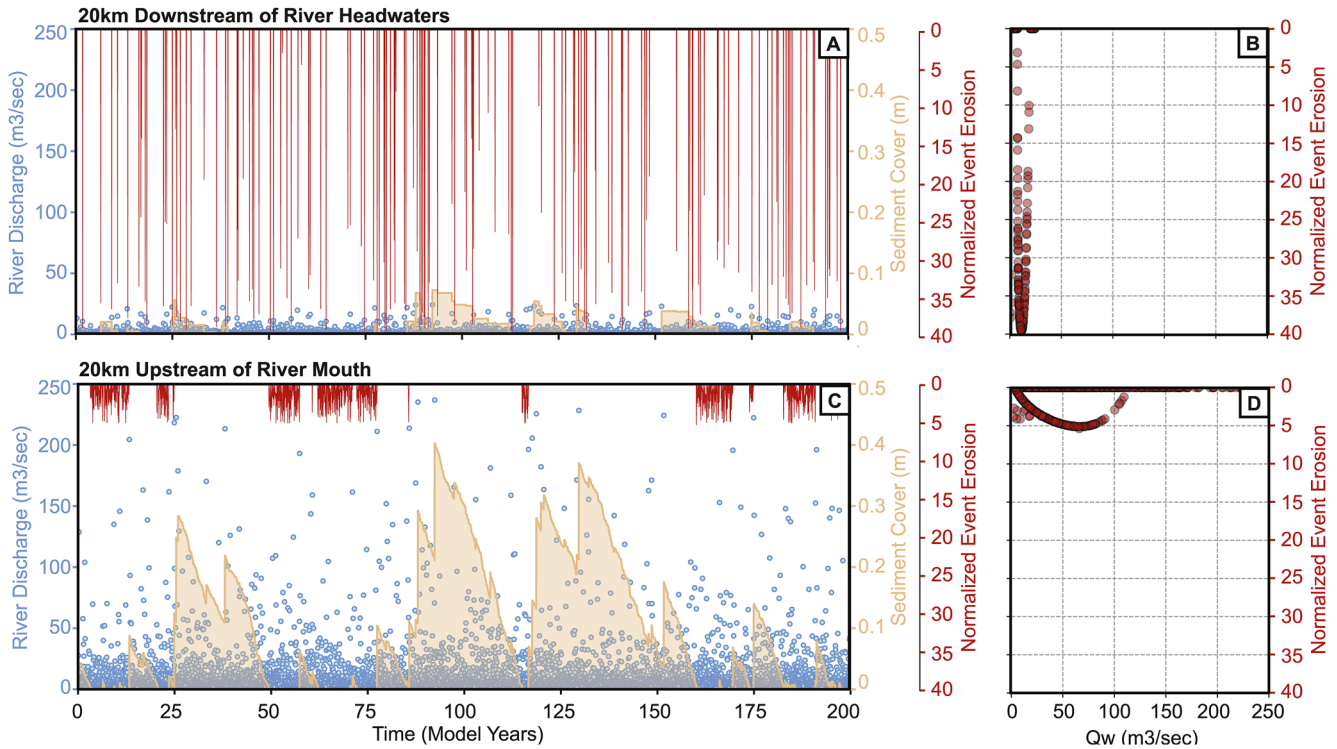

Figure 4. Two time series of water discharge (blue dots), sediment cover (tan line), and normalized event incision (red line). Normalized event incision is the bedrock incision which occurs during a timestep divided by the rock uplift which occurs during that timestep. Model results are for a river with a low rate of rock uplift (0.1 mm/yr), high river discharge variability ($k_v = 0.3$), and high sediment supply sensitivity ($\eta = 2.0$) (a) Model results from a node 20 km downstream of model headwaters. (b) Model results from a node 20 km upstream of model river mouth.

3. Results

3.1. Basic Model Behavior

In Figure 4 we show the behavior of our model at dynamic equilibrium at two nodes, one 20 km downstream of the channel head and one 20 km upstream of the channel mouth. In these simulations, water discharge variability is low ($k_v = 3.0$). We plot water discharge and event normalized incision, defined as bedrock erosion which occurs during a timestep normalized by the rock uplift which occurs during a timestep, through time. For models in dynamic equilibrium, long-term rates of bedrock incision are equal to the rock uplift rate. Were river incision steady in time, this metric would always be equal to one. The model captures differences in channel response to sediment input along the length of the model river. In the headwaters, individual sediment supply events are evident in the time series of sediment cover and river incision, while near the river mouth these signals are shredded and we observe longer-duration pulses of sediment cover (Jerolmack & Paola, 2010).

3.2. Impact of Water and Sediment Variability

Figure 5 shows four different model scenarios at dynamic equilibrium, all with the same rate of rock uplift ($U_r = 5$ mm/yr) and grain sizes. Figure 5 and all subsequent model results plot data from 20 km upstream of the model river mouth. Figures 5a and 5b have low sediment sensitivity. In these cases, we see the response to increasingly variable river discharge that would be expected in a standard stochastic formulation of the SPIM. As river discharge variability increases from Figures 5a to 5b, we see a decrease in the number of events which erode bedrock but an increase in peak rates of river incision during large events. This supports existing theory regarding discharge variability in threshold dominated bedrock rivers (DiBiase & Whipple, 2011; Molnar et al., 2006), where increasing discharge variability increases the erosive power of rare large storms.

Comparing Figure 5a against Figure 5c isolates the impact of changing sediment supply sensitivity while keeping water discharge variability low. Here we see relatively little impact of changing sediment supply sensitivity.

10.1029/2023JF007148

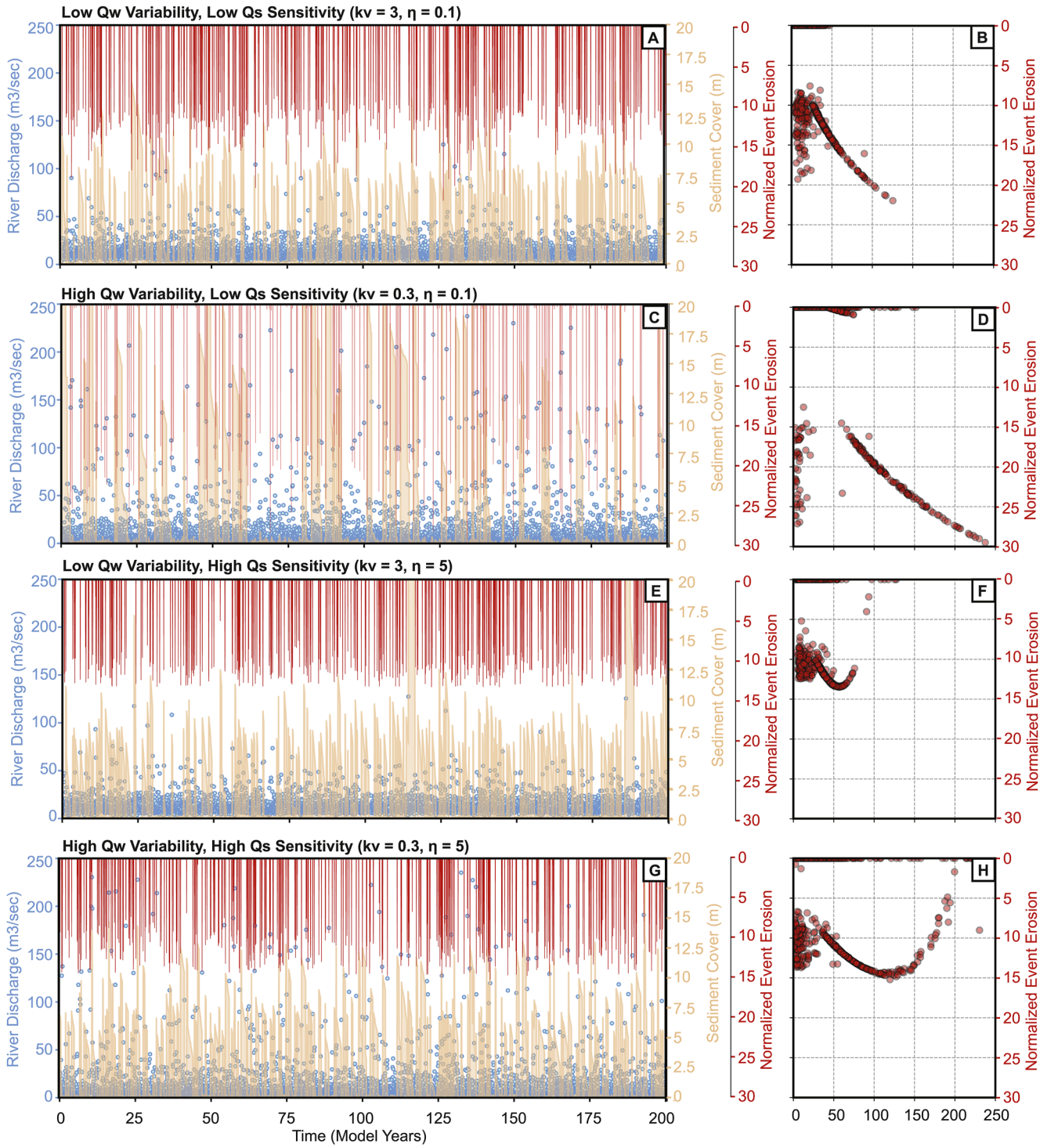

Figure 5. Four time series of river discharge, sediment cover, and normalized event incision for different endmember scenarios of water discharge (Q_w) variability and sediment supply (Q_s) sensitivity. Results are plotted for a model node 20 km upstream of the model river mouth. All models have constant rock uplift of 5 mm/yr. A shows results from a model run with low Q_w and Q_s variability, D from a model run with high Q_w and Q_s variability, and B and C have combinations of low and high variability.

In Figure 5c, increased sediment supply sensitivity drives slightly lower peak incision rates relative to those in Figure 5a. We see a stronger impact of sediment supply sensitivity by comparing Figure 5b with Figure 5d. Here, there is high water discharge variability in both cases, with Figure 5b having low sediment sensitivity and

Figure 5d having high sediment sensitivity. The high sediment sensitivity case has markedly lower peak incision rates because sediment supply to channels is concentrated into rare large events, and thus the bedrock exposure fraction (F from Equation 3) approaches or equals zero during the largest discharge events. This result suggests that incision rates do not always increase monotonically with increasing discharge variability.

The previous point is well illustrated by comparing Figure 5c with Figure 5d. In doing so, we isolate the impact of changing river discharge variability while sediment supply sensitivity remains high. Note that there is relatively little impact of changing river discharge variability on peak rates of bedrock incision or on the frequency of bedrock incision, but strong differences between Figures 5a and 5b where sediment supply variability is low.

In Figure 6, we plot time series of our model at equilibrium for the same four endmember scenarios as in Figure 5 but with a rock uplift rate of 0.1 mm/yr. The patterns of river incision response to the combined forcing of river discharge variability and sediment supply sensitivity are the same for the low rock uplift models as for the high rock uplift rate models. Introducing high sensitivity sediment supply in which sediment is delivered concurrently with the largest storms decreases peak incision rates and forces the river to accomplish more of its geomorphic work during moderately sized storms. Peak normalized event incision rates are lower in Figure 6 than in Figure 5, owing to lower channel slopes due to slower rock uplift. The magnitude of sediment cover is far lower in these slower uplift models because long-term sediment availability is 50× lower for a basin uplifting at 0.1 mm/yr than one uplifting at 5 mm/yr (Equation 15).

3.3. An Upper Threshold for River Incision

We quantify the contribution of floods of different sizes to total geomorphic work in varied discharge and sediment supply regimes in Figure 7. In models with no sediment (Figures 7a and 7b), average incision during a given event (point colors) increases monotonically with river discharge. Rivers respond as expected to increasingly variable discharge, where more variable systems see increased importance of the rarest events while less variable systems are dominated by more common events. The tails of the PDF of Q_w are longer in the high discharge variability system, but we plot them on the same x-axes for comparability. No discharge events occur within the gray-shaded areas.

In Figures 7c and 7d, we add low sensitivity ($\eta = 0.25$) sediment supply. We see little impact of this addition on distributions of bedrock river incision and partitioning of geomorphic work. It is often assumed that the threshold for river incision is set by the threshold for grain motion. If this is the case, we expect little difference in river behavior comparing one model with an imposed threshold against another model with near-constant sediment supply. This is supported by the agreement between models with no sediment (Figures 7a and 7b) and those with low sensitivity sediment supply (Figures 7c and 7d).

High sediment supply sensitivity ($\eta = 2.0$), however, greatly impacts the behavior of our model rivers. In Figures 7e and 7f, high sediment supply sensitivity focuses sediment delivery into the largest events. This decreases the importance of those rare large events to bedrock river incision and increases the importance of the moderately sized frequently occurring events. Peak average rates of incision during events decrease, and the relationship between average incision during an event and event size becomes non-monotonic. Small events do little or no geomorphic work, and incision rates increase as water discharge increases, but when water discharge is high enough, sediment supply overwhelms sediment transport capacity, bedrock exposure decreases, and event incision rates fall. In the largest events, sediment supply far exceeds sediment transport capacity and no erosion occurs.

An important observation from Figure 7 is that partitioning of geomorphic work across the distribution of river discharge events is non-unique when both water and sediment sensitivity are accounted for. Comparing Figures 7c and 7f we see that the partitioning of geomorphic work (locations of scatter points) is roughly the same even though the distribution of Q_w and the patterns in average incision rates (point colors) across this distribution are quite different. Geomorphic work in Figure 7c is concentrated into the moderately sized common events because water discharge is low variability and sediment supply is low sensitivity. When the tails of the Q_w distribution are short and sediment supply is near constant, the frequent common events do most of the geomorphic work. Geomorphic work in Figure 7f is also concentrated into the moderately sized common events because although it has highly variable river discharge, the concentration of sediment supply into rare large events decreases the impact of these events. This suggests that bedrock rivers in two landscapes which are uplifting at the same rate but seem to be as different as possible—low water variability and sediment sensitivity versus high water variability and sediment supply sensitivity—may accomplish their geomorphic work in remarkably similar ways in terms of which event magnitudes accomplish the most bedrock incision.

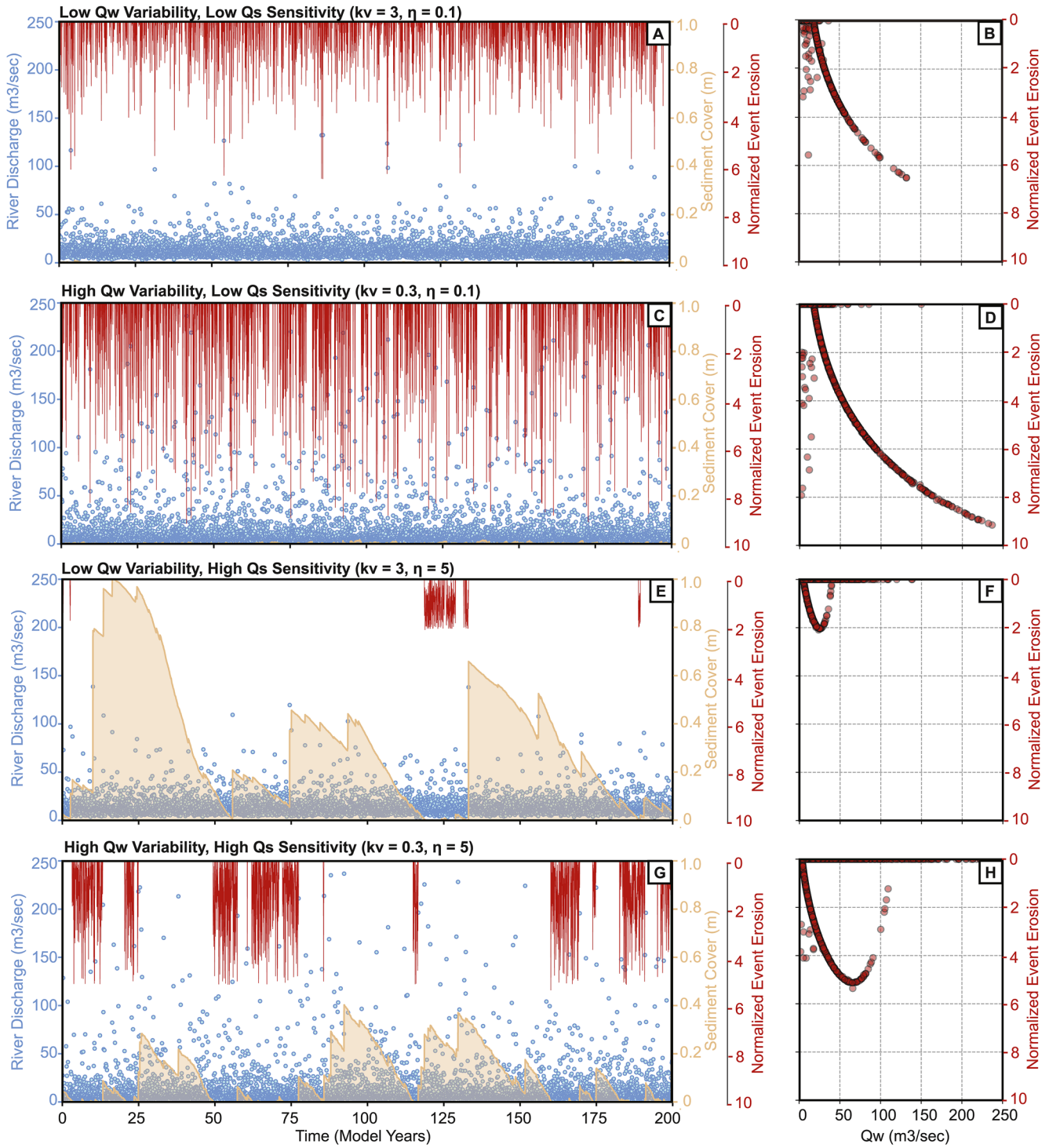

Figure 6. Four time series of river discharge, sediment cover, and normalized event incision for endmember scenarios of water discharge (Q_w) variability and sediment supply (Q_s) sensitivity. Results are plotted for a model node 20 km upstream of the model river mouth. All models have constant rock uplift of 0.1 mm/yr. Panels here are organized by endmember variability scenarios (Figure 5).

This complicates our understanding of bedrock river incision in response to climatic forcings and suggests the need for study of the dynamics of hillslope sediment supply to channels over both event and geomorphic timescales.

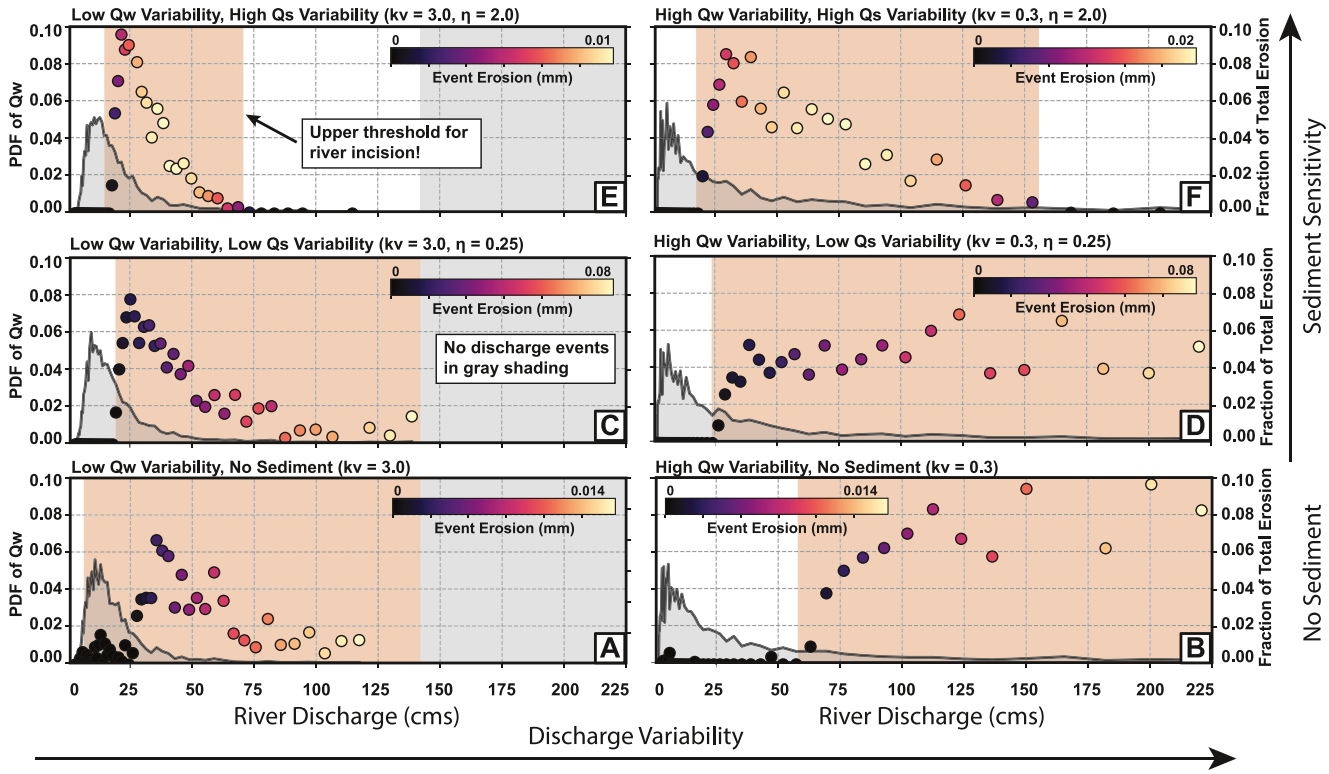

Figure 7. Impact of covarying river discharge variability and sediment supply sensitivity on the partitioning of geomorphic work across a distribution of river discharge events. Each plot shows a PDF of river discharge (gray line and shading, left *y*-axis), scatter points are located by the fraction of total incision (right *y*-axis) accomplished by floods of that magnitude, where we split floods into 60 log-distributed magnitude bins. Points are colored by the average bedrock erosion accomplished by an event in each bin (we call this event erosion). The left column of the figure has low water discharge variability ($k_v = 3.0$), and the right column has high discharge variability ($k_v = 0.3$). Sediment supply sensitivity increases from the bottom row of the figure to the top. Panels (a) and (b) have no sediment, and instead we apply a threshold for incision equal to the threshold of grain motion using the same grain size patterns as the sediment cover models. Panels (c) and (d) have low sediment supply sensitivity ($\eta = 0.25$), and (e) and (f) have high sediment supply sensitivity ($\eta = 2.0$). All models here are at dynamic equilibrium with 0.1 mm/yr rock uplift. Orange shading shows the range of discharge events in which erosion occurs.

3.4. Impact on Channel Morphology

We compare the morphology of model channels using ratios of channel slope to channel width. In Figure 8, we show the combined impact of water discharge and sediment supply variability on channel morphology for low (0.1 mm/yr) and high (5 mm/yr) rock uplift rates. We normalize this parameter by its lowest measured value for each uplift rate to allow comparison between the two panels in Figure 8. Non-normalized values of channel slope and width are available in Supporting Information S1.

In Figure 8 we push η to higher and lower values than before, ranging from 0.1 to 5.0. We observe that our nondimensional morphology parameter decreases with increasing variable water discharge. This is expected from current theory, which predicts lower channel steepness as discharge is increasingly variable (DiBiase & Whipple, 2011). We see little impact of sediment supply sensitivity η for the case of low rock uplift rates (Figure 8b). We observe, however, a strong impact of sediment supply sensitivity on channel morphology when rock uplift rates are high (Figure 8a). As we increase η under high rates of rock uplift, channels get less steep and/or achieve greater widths. We note that channel slope and width are readily measured either in the field or remotely, thus presenting a feasible path toward validating these model predictions.

4. Discussion

The model results presented here show the importance of sediment supply sensitivity to precipitation events in controlling river dynamics in actively eroding landscapes. Given the ubiquity of time-varying hillslope sediment supply across landscapes, consideration of sediment supply sensitivity is necessary to fully link river process and form over geologic timescales. Current modeling frameworks largely ignore this complexity, potentially

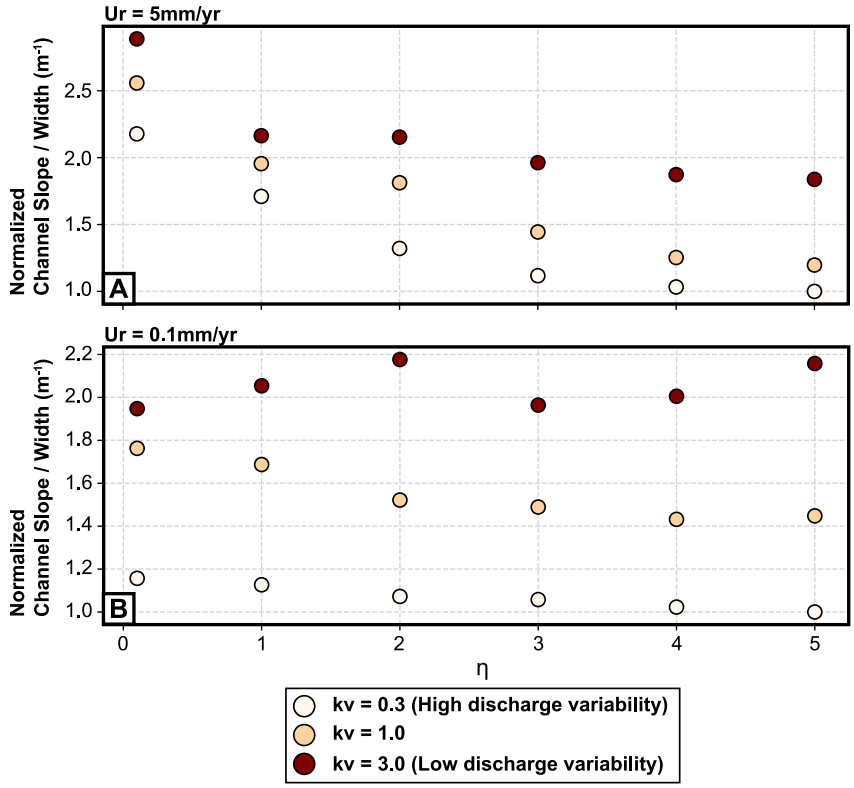

Figure 8. Channel slope divided by channel width (m^{-1}) plotted against sediment sensitivity η for high (panel a) and low (panel b) uplift scenarios. Values are normalized by lowest value for each uplift rate to improve comparability between panels (a) and (b).

mischaracterizing how tectonics and climate imprint themselves on landscape form. Below we present our evidence for the presence of an upper threshold for river incision for systems where sediment supply is highly sensitive to runoff events, and discuss implications for the observation of bedrock incision magnitudes, the importance of rock uplift rate, model caveats, and directions for future work.

4.1. Evidence of an Upper Threshold for Bedrock Incision

To show the tradeoff between sediment supply and sediment transport capacity in our model, we plot sediment supply Q_s^* from Equation 13 and sediment transport capacity Qt^* from Equation 9 in Figure 9. We plot these two variables against a distribution of nondimensional water discharge (Q_w^*) from Equation 11 for endmember values of k_v and η. This plot illustrates the transition from net incision to net aggradation during individual weather events, defining an important threshold beyond which incision no longer occurs due to sediment cover.

Scenarios in Figures 9a and 9b have high sediment supply sensitivity ($\eta = 2.0$). In the high sediment supply sensitivity scenarios, the majority of hillslope sediment supply occurs during rare large events. As such, the smallest events receive less sediment and thus their sediment transport capacities are higher than sediment supply, which allows bedrock erosion to occur. The largest events have sediment supply that significantly exceeds their transport capacity. Discharge events become depositional above this threshold where the tan and black lines cross in Figures 9a and 9b. This behavior is seen in nature during large storms in steep landscapes (DeLisle et al., 2021; Kim et al., 2021; Webb et al., 2008; Yanites et al., 2018) or after wild fires (Anderson et al., 2015; Rengers et al., 2020), where the loss of hillslope cohesion effectively increases the local value of η for a period of time.

Figures 9c and 9d shows scenarios with low sediment supply sensitivity ($\eta = 0.25$). Here, the most frequent discharge events, which are lower than long-term mean river discharge, drive sediment aggradation. These events have low sediment supply to channels but even lower sediment transport capacity. As river discharge increases, sediment transport capacity exceeds hillslope sediment supply and rivers begin to erode bedrock. This fits the

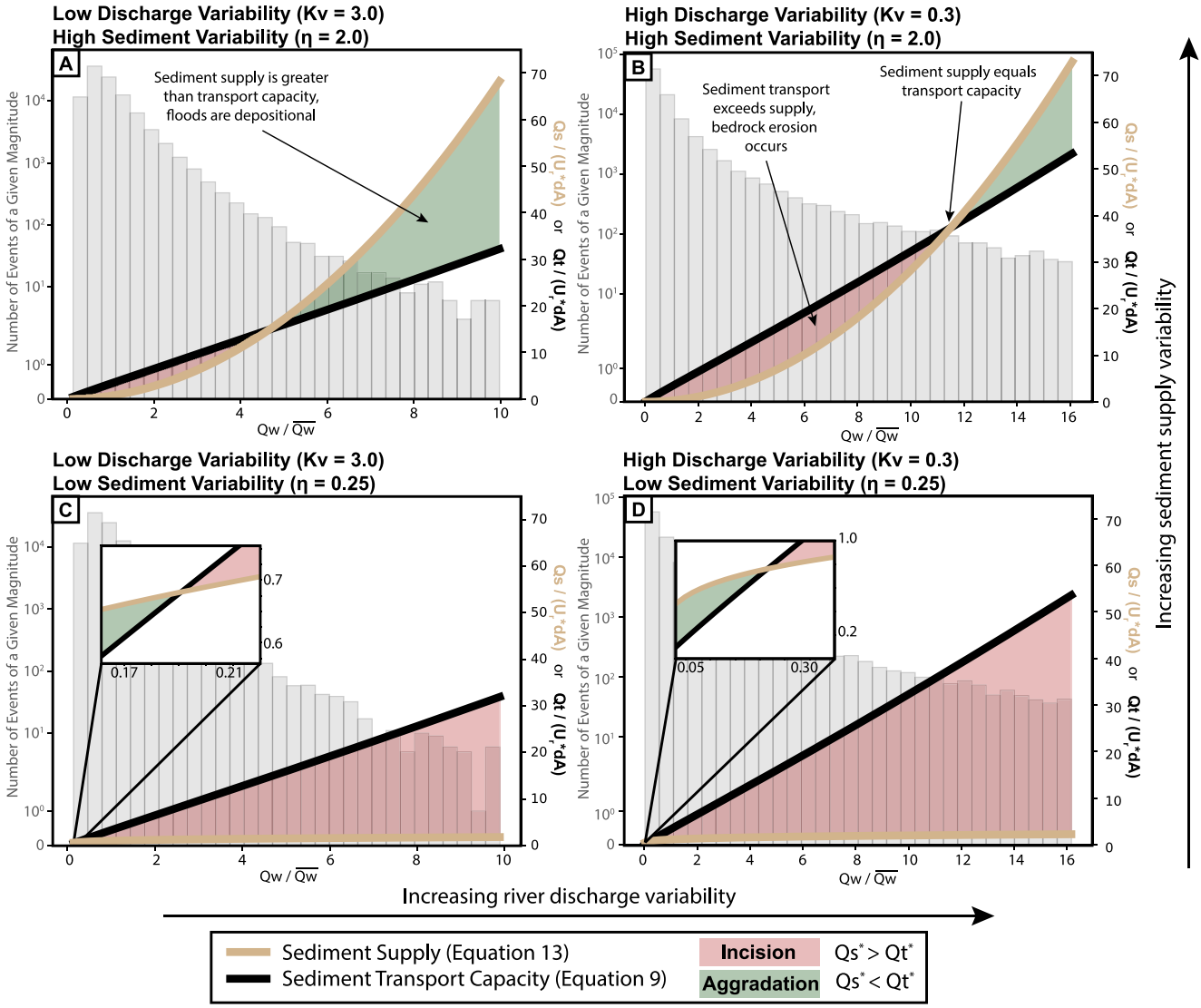

Figure 9. Relationships between sediment supply (Q_s, tan line) and transport capacity (Q_t, black line) plotted against Q_w for endmember variability scenarios. The histogram shows the number of events of a given size for a random sampling of 100,000 events from these controlling parameters. Note the log-scale on the *y*-axis for histogram counts. Sediment supply and transport are both normalized by the product of rock uplift (U_r) and contributing drainage area (dA), which is the total available sediment volume. In the red shaded area, events have greater sediment transport capacity than sediment delivery. In the green shaded area, sediment supply exceeds transport capacity. Histogram shows the counts of events of a given magnitude. Note the log-scale on the *y*-axis for histogram counts.

current understanding of how rivers behave in response to variable river discharge, in which a threshold of discharge and shear stress must be overcome to erode bedrock. Above this threshold, river incision is expected to increase monotonically with increasing discharge. Note that this threshold is larger than the threshold for grain size entrainment as it also encapsulates the need to transport the total supplied bedload.

These findings have implications for hillslope-channel coupling and landscape evolution. As relief evolves in an orogen, hillslopes are likely to become more susceptible to landslides and stochastic hillslope events. Thus, hillslope response to large storms and sediment supply variability will change through the development of relief in an evolving landscape. Any attempt to account for such effects in a strictly stream power framework (i.e., $E = KA^mS^n$) would have to parametrize changes in erosional efficiency (K) with relief development or through time. The importance of hillslope-channel coupling also has implications for considering landscape response to climate change. In short, the model results here show that increases in storminess might not increase river erosional efficiency as the result depends on how hillslopes and their sediment supply sensitivity are impacted by climate changes. Such feedbacks within the landscape system could explain why impacts of climate change on landscape evolution remain enigmatic.

4.2. Implications for River Morphology and Incision Rates

Observation of natural systems suggests that the sediment supply sensitivity is fundamental to understanding bedrock river evolution. Many mountain rivers are consistently inundated with sediment over the timescales of human observation, even as geomorphic evidence clearly points to active river incision over geologic time (Blöthe & Korup, 2013; Yanites et al., 2011). Strath terrace development requires cyclical periods of aggradation and incision to form even in highly active landscapes (Finnegan et al., 2014; Fuller et al., 2009; Hancock & Anderson, 2002). Sediment cover is observed to change rapidly in mountain rivers with frequent observations of significant aggradation following large storm events (DeLisle et al., 2021; Kim et al., 2021; Pfeiffer et al., 2019; Webb et al., 2008), though this can result from both increases and decreases in sediment cover (Turowski et al., 2013).

The results presented here also have implications for interpreting event-scale magnitudes of incision. The observed nonmonotonic relationship between river discharge and bedrock erosion when sediment supply sensitivity is accounted for suggests the presence of a feedback that limits incision rates in fast-eroding landscapes during rare, large events. In these endmember cases where hillslope erosion and river incision rates are high, hillslopes provide enough sediment to channels to limit the rate of erosion of fresh bedrock. Rivers in these landscapes must incise bedrock quickly during periods of bedrock exposure in channels to make up for periods of sediment cover and keep up with rock uplift through geomorphic time. This conclusion is supported by field observations of extremely fast bedrock river incision during even moderate storms in active orogens (Hancock et al., 1998; Hartshorn et al., 2002; Johnson et al., 2010). This conclusion suggests the need to improve our integrated understanding of hillslope-fluvial systems, especially in areas with high sediment flux and those which are dominated by mass wasting processes.

4.3. The Impact of Rock Uplift Rate

Rock uplift plays a dual role in controlling sediment supply variability. In our model, rock uplift rate determines long-term sediment supply ($\overline{Q_s}$ in Equation 15), so increasing rock uplift rate increases total sediment load. We hypothesize a second impact of rock uplift, in which increasing rock uplift rate increases sediment supply sensitivity (η in Equation 13). Evidence for this hypothesis exists in that widespread concurrent landslide initiation is observed only in steep landscapes which have relatively high rates of rock uplift (DeLisle et al., 2021; Kim et al., 2021; Marc et al., 2018; Roback et al., 2017; Webb et al., 2008). As rock uplift rates increase, hillslopes steepen and shift their sediment delivery styles from diffusive to mass-wasting, causing increasingly variable sediment delivery.

4.4. Range of Chosen η Values

We use a power-law relationship between nondimensional river discharge and nondimensional sediment supply (Equation 13). While the true relationship between these variables is an important unconstrained parameter in understanding sediment delivery to and transport through mountain rivers, we believe that our chosen range of η values from 0.1 to 5.0 represents a wide range of possible real-world behaviors. As η approaches zero, sediment supply approaches a constant rate. This is the simplest form of a river discharge—sediment supply relationship. We use a $\eta \geq 2.0$ to represent systems like that of southern Taiwan in which extreme sediment supply events have been observed which are many orders of magnitude greater than long-term geomorphic averages (DeLisle et al., 2022). For example, Typhoon Morakot produced rainfall in excess of 3,000 mm (Chien & Kuo, 2011), which is roughly an order of magnitude greater than typhoons of average size in the region. Using a value of $\eta = 2.0$, our model would predict sediment delivery of 100× background rates during this storm, which to a first order agrees with published observations (DeLisle, et al., 2022). We acknowledge, however, that there is a strong need for continued study to better constrain the relationship between river discharge and sediment supply at the event scale.

4.5. Assumptions and Caveats

In the model results presented here, we keep many of the constituent variables (e.g., K in Equation 2, D_o in Equation 10, k_w in Equation 17, C_h and H_e in Equation 19) constant across model runs. Each of these variables

likely exerts a control on the equilibrium morphology of our model rivers. K is important in setting channel slope (Whipple & Tucker, 1999), grain size is known to modify channel steepness (Lai et al., 2021), k_w controls the variability of channel widths, and the variables in Equation 19 determine drainage area which controls both river discharge and sediment supply. In the initial presentation of this model, we have chosen to keep these variables constant and focus on the impacts of water discharge and sediment supply sensitivity. Although outside the scope of this paper, each of these variables deserves independent study within this new modeling framework.

Our model does not explicitly account for the tools effect where increasing sediment load in bedrock rivers drives increasing rates of bedrock erosion (Sklar & Dietrich, 2004, 2006). We have chosen to represent only the cover effect for simplicity in the presentation of this model but believe that adding a tools effect would either strengthen or leave unchanged the results presented here. The cover effect in this modeling framework occurs when large, rare discharge events drive high volumes of sediment supply. By adding a tools effect, the smaller sediment supply at moderate discharges may accelerate erosion due to the increase in available tools, but large events accompanied by large volumes of sediment would still be depositional rather than erosional.

We recognize the importance of choosing an appropriate time step in the proper application of this model. We sample discharge events from a daily distribution and stretch the impact of those events and the sediment supply resultant from them over the duration of a timestep. This method has been tested and shown to be effective for processes of detachment limited bedrock river incision (Shen et al., 2021; Tucker & Bras, 2000), but we acknowledge that the nonlinearity of our model makes assuming the same is true here complicated. If one was to use this model with $dt = 1$ year, for example, the largest sediment supply events would drive 24× greater sediment delivery than they do when we use our dt of 1/24 year. We chose $dt = 1/24$ year as a balance between high enough resolution to accurately capture stochastic events driven by weather, while maintaining computational efficiency.

Our model results are concerned primarily with the impact of local sediment supply from hillslopes to adjacent channels during individual storm events. We do not directly quantify the impact of waves of sediment which propagate downstream after deposition. The impact of downstream-propagating sediment can be seen, however, in Figures 4–6. In the scatter plots in these figures, our results show a number of events which accomplish no bedrock incision even with relatively large river discharge. This occurs in times of sediment cover resulting from previous upstream depositional events, as sediment is removed from the system. Our results are primarily concerned with the non-zero events, however, and these trends are not impacted by these periods of sediment cover.

4.6. Future Work

In Figure 8, we presented trends in channel morphology driven by the sediment sensitivity exponent η. Our model predicts a strong effect of η on channel morphology, especially in rapidly uplifting landscapes. The fundamental prediction from Figure 8 is that in rapidly uplifting landscapes, increasingly variable sediment supply should drive lower channel slopes and wider channels. This is an important observation, as sediment supply is a largely unconstrained parameter across evolving orogens. Future work should seek to constrain η using model predictions of channel morphology in tandem with available observations of hillslope sediment supply in response to precipitation events across landscapes with a range of sediment delivery styles. Our model represents time-varying sediment supply but does not account for point-source inputs of sediment. In natural systems, sediment delivery is often highly spatially varied on short timescales, especially when sediment delivery occurs predominantly via mass-wasting. Our model could be expanded to include these effects, and doing so may introduce new feedbacks between hillslope and fluvial processes.

Our results suggest that the style and timing of hillslope sediment transport act as a first order control on patterns of river incision. While we tested a range of values for η, we believe constraining this variable through field and modeling studies to be an important direction toward better calibrating models of bedrock river evolution. We intuitively suggest that lower values of η be used for landscapes dominated by slow moving diffusing processes such as soil creep and frost heave. Higher values of η best represent landscapes dominated by mass wasting processes like landslides and debris flows, where sediment supply is dominated by rare, large magnitude events. It is possible that η varies temporally on both short and long timescales. On short timescales, η should almost certainly increase following earthquakes and forest fires, as decreased cohesion in soils commonly leads to outsized landslide triggering and debris flow initiation during the first rainstorms after fires and earthquakes.

Over long timescales, η likely varies during orogenesis as landscapes steepen and hillslopes transition from diffusive hillslope sediment supply to mass wasting processes.

5. Conclusions

By incorporating the impact of sediment supply sensitivity to precipitation events into a model for bedrock river incision by stochastic water discharge, we uncover a complicated picture of stochastic river evolution. We show that the simplest relationships between river discharge and bedrock erosion, normally assumed to be monotonic and positive, may not be so. Addition of time-variable sediment supply to a stochastic model for bedrock river incision can limit the geomorphic work accomplished during the largest floods. This effect strongly complicates river response to discharge variability but offers an important new framework to consider hillslope-channel coupling in landscape evolution. The evidence presented here indicates that hillslope sediment supply is a significant control on river evolution, especially in landscapes with highly variable hillslope processes, which deserves the same careful study given to river discharge.

Conflict of Interest

The authors declare no conflicts of interest relevant to this study.

Data Availability Statement

The python script (version 1.0.0) used in producing these numerical models, along with some basic plotting functions, is available via Zenodo at https://doi.org/10.5281/zenodo/8125005 (DeLisle & Yanites, 2023).

Acknowledgments
This work was supported by U.S. National Science Foundation Grant EAR-1727736 to B. Yanites. C. DeLisle was supported by the Department of Defense National Science and Engineering Graduate Fellowship.

References

Anderson, S. W., Anderson, S. P., & Anderson, R. S. (2015). Exhumation by debris flows in the 2013 Colorado Front Range storm. *Geology*, *1*(5), 391–394. https://doi.org/10.1130/G36507.1

Blöthe, J. H., & Korup, O. (2013). Millennial lag times in the Himalayan sediment routing system. *Earth and Planetary Science Letters*, *382*, 38–46. https://doi.org/10.1016/j.epsl.2013.08.044

Bull, W. B. (1979). Threshold of critical power in streams. *Geological Society of America Bulletin*, *90*(5), 453–464. https://doi.org/10.1130/0016-7606(1979)90<453:tocpis>2.0.co;2

Campforts, B., Shobe, C. M., Overeem, I., & Tucker, G. E. (2022). The art of landslides: How stochastic mass wasting shapes topography and influences landscape dynamics. *Journal of Geophysical Research: Earth Surface*, *127*(8), e2022JF006745. https://doi.org/10.1029/2022JF006745

Campforts, B., Shobe, C. M., Steer, P., Vanmaercke, M., Lague, D., & Braun, J. (2020). HyLands 1.0: A hybrid landscape evolution model to simulate the impact of landslides and landslide-derived sediment on landscape evolution. *Geoscientific Model Development*, *13*(9), 3863–3886. https://doi.org/10.5194/gmd-13-3863-2020

Chen, S.-A., Michaelides, K., Grieve, S. W. D., & Singer, M. B. (2019). Aridity is expressed in river topography globally. *Nature*, *573*, 573–577. https://doi.org/10.1038/s41586-019-1558-8

Chien, F.-C., & Kuo, H.-C. (2011). On the extreme rainfall of Typhoon Morakot (2009). *Journal of Geophysical Research*, *116*(D5), D05104. https://doi.org/10.1029/2010JD015092

Cowie, P. A., Whittaker, A. C., Attal, M., Roberts, G., Tucker, G. E., & Ganas, A. (2008). New constraints on sediment-flux–dependent river incision: Implications for extracting tectonic signals from river profiles. *Geology*, *36*(7), 535–538. https://doi.org/10.1130/G24681A.1

Crave, A., & Davy, P. (2001). A stochastic "precipiton" model for simulating erosion/sedimentation dynamics. *Computers & Geosciences*, *27*(7), 815–827. https://doi.org/10.1016/S0098-3004(00)00167-9

Deal, E., Favre, A.-C., & Braun, J. (2017). Rainfall variability in the Himalayan orogen and its relevance to erosion processes. *Water Resources Research*, *53*(5), 4004–4021. https://doi.org/10.1002/2016WR020030

DeLisle, C., & Yanites, B. J. (2023). Data for 'rethinking variability in bedrock rivers: Sensitivity of hillslope sediment supply to precipitation events modulates bedrock incision during floods' July 7, 2023 release (version 1.1.0) [Software]. Zenodo. https://doi.org/10.5281/zenodo/8125005

DeLisle, C., Yanites, B. J., Chen, C.-Y., Shyu, B. H., & Rittenour, T. M. (2021). Extreme event-driven sediment aggradation and erosional buffering along a tectonic gradient in southern Taiwan. *Geology*, *50*(1), 16–20. https://doi.org/10.1130/G49304.1

DeLisle, C., Yanites, B. J., Chen, C. Y., Shyu, J. B. H., & Rittenour, T. M. (2022). Extreme event-driven sediment aggradation and erosional buffering along a tectonic gradient in southern Taiwan. *Geology*, *50*(1), 16–20. https://doi.org/10.1130/g49304.1

DiBiase, R. A., & Whipple, K. X. (2011). The influence of erosion thresholds and runoff variability on the relationships among topography, climate, and erosion rate. *Journal of Geophysical Research*, *116*(F4), F04036. https://doi.org/10.1029/2011JF002095

Duvall, A., Kirby, E., & Burbank, D. (2004). Tectonic and lithologic controls on bedrock channel profiles and processes in coastal California. *Journal of Geophysical Research*, *109*(F3), F03002. https://doi.org/10.1029/2003JF000086

Exner, F. M. (1920). *Zur physik der dünen*. Hölder.

Exner, F. M. (1925). Uber die wechselwirkung zwischen wasser und geschiebe in flussen. *Akademie der Wissenschaften in Wien Mathematisch-Naturwissenschaftliche Klasse, Abteilung III*, *134*, 165–203.

Ferrier, K. L., Huppert, K. L., & Perron, J. T. (2013). Climatic control of bedrock river incision. *Nature*, *496*(7444), 206–209. https://doi.org/10.1038/nature11982

Finnegan, N. J., Schumer, R., & Finnegan, S. (2014). A signature of transience in bedrock river incision rates over timescales of 104–107 years. *Nature*, *505*(7483), 391–394. https://doi.org/10.1038/nature12913

Forte, A. M., Leonard, J. S., Rossi, M. W., Whipple, K. X., Heimsath, A. M., Sukhishvili, L., et al. (2022). Low variability runoff inhibits coupling of climate, tectonics, and topography in the Greater Caucasus. *Earth and Planetary Science Letters*, *584*, 117525. https://doi.org/10.1016/j.epsl.2022.117525

Fuller, T. K., Perg, L. A., Willenbring, J. K., & Lepper, K. (2009). Field evidence for climate-driven changes in sediment supply leading to strath terrace formation. *Geology*, *37*(5), 467–470. https://doi.org/10.1130/G25487A.1

Hack, J. T. (1957). *Studies of longitudinal stream profiles in Virginia and Maryland*. U.S. Government Printing Office.

Hancock, G. S., & Anderson, R. S. (2002). Numerical modeling of fluvial strath-terrace formation in response to oscillating climate. *Geological Society of America Bulletin*, *114*(9), 1131–1142. https://doi.org/10.1130/0016-7606(2002)114<1131:NMOFST>2.0.CO;2

Hancock, G. S., Anderson, R. S., & Whipple, K. X. (1998). Beyond power: Bedrock river incision process and form. In K. J. Tinkler & E. E. Wohl (Eds.), *Rivers over rock: Fluvial processes in bedrock channels* (pp. 35–60). American Geophysical Union. https://doi.org/10.1029/GM107p0035/summary

Hartshorn, K., Hovius, N., Dade, W. B., & Slingerland, R. L. (2002). Climate-driven bedrock incision in an active mountain belt. *Science*, *297*(5589), 2036–2038. https://doi.org/10.1126/science.1075078

Jerolmack, D. J., & Paola, C. (2010). Shredding of environmental signals by sediment transport. *Geophysical Research Letters*, *37*(19), 1–5. https://doi.org/10.1029/2010GL044638

Johnson, J. P. L., Whipple, K. X., & Sklar, L. S. (2010). Contrasting bedrock incision rates from snowmelt and flash floods in the Henry Mountains, Utah. *GSA Bulletin*, *122*(9–10), 1600–1615. https://doi.org/10.1130/B30126.1

Johnson, J. P. L., Whipple, K. X., Sklar, L. S., & Hanks, T. C. (2009). Transport slopes, sediment cover, and bedrock channel incision in the Henry Mountains, Utah. *Journal of Geophysical Research*, *114*(F2), F02014. https://doi.org/10.1029/2007JF000862

Kim, J., Woo, K. S., Lee, K. C., & Sohn, Y. K. (2021). Overnight formation of a bouldery alluvial fan by a torrential rain in a granitic mountain (Mt. Seoraksan, Republic of Korea). *The Sedimentary Record*, *19*(2), 5–11. https://doi.org/10.2110/sedred.2021.2.2

Kirby, E., & Whipple, K. (2001). Quantifying differential rock-uplift rates via stream profile analysis. *Geology*, *29*(5), 415–418. https://doi.org/10.1130/0091-7613(2001)029<0415:QDRURV>2.0.CO;2

Kirby, E., & Whipple, K. X. (2012). Expression of active tectonics in erosional landscapes. *Journal of Structural Geology*, *44*, 54–75. https://doi.org/10.1016/j.jsg.2012.07.009

Lague, D. (2010). Reduction of long-term bedrock incision efficiency by short-term alluvial cover intermittency. *Journal of Geophysical Research*, *115*(F2), 23. https://doi.org/10.1029/2008JF001210

Lague, D. (2014). The stream power river incision model: Evidence, theory and beyond. *Earth Surface Processes and Landforms*, *39*(1), 38–61. https://doi.org/10.1002/esp.3462

Lague, D., Hovius, N., & Davy, P. (2005). Discharge, discharge variability, and the bedrock channel profile. *Journal of Geophysical Research*, *110*(F4), F04006. https://doi.org/10.1029/2004JF000259

Lai, L. S.-H., Roering, J. J., Finnegan, N. J., Dorsey, R. J., & Yen, J.-Y. (2021). Coarse sediment supply sets the slope of bedrock channels in rapidly uplifting terrain: Field and topographic evidence from eastern Taiwan. *Earth Surface Processes and Landforms*, *46*(13), 2671–2689. https://doi.org/10.1002/esp.5200

Lamb, M. P., Dietrich, W. E., & Sklar, L. S. (2008). A model for fluvial bedrock incision by impacting suspended and bed load sediment. *Journal of Geophysical Research*, *113*(F3), F03025. https://doi.org/10.1029/2007JF000915

Leopold, L. B., & Maddock, T. (1953). *The hydraulic geometry of stream channels and some physiographic implications*. U.S. Government Printing Office.

Marc, O., Stumpf, A., Malet, J.-P., Gosset, M., Uchida, T., & Chiang, S.-H. (2018). Initial insights from a global database of rainfall-induced landslide inventories: The weak influence of slope and strong influence of total storm rainfall. *Earth Surface Dynamics*, *6*(4), 903–922. https://doi.org/10.5194/esurf-6-903-2018

Meyer-Peter, E., & Müller, R. (1948). Formulas for bed-load transport.

Molnar, P., Anderson, R. S., Kier, G., & Rose, J. (2006). Relationships among probability distributions of stream discharges in floods, climate, bed load transport, and river incision. *Journal of Geophysical Research*, *111*(F2), F02001. https://doi.org/10.1029/2005JF000310

Paola, C., & Voller, V. R. (2005). A generalized Exner equation for sediment mass balance. *Journal of Geophysical Research*, *110*(F4), 8. https://doi.org/10.1029/2004JF000274

Perron, J. T., & Royden, L. (2013). An integral approach to bedrock river profile analysis. *Earth Surface Processes and Landforms*, *38*(6), 570–576. https://doi.org/10.1002/esp.3302

Pfeiffer, A. M., Collins, B. D., Anderson, S. W., Montgomery, D. R., & Istanbulluoglu, E. (2019). River bed elevation variability reflects sediment supply, rather than peak flows, in the uplands of Washington state. *Water Resources Research*, *55*(8), 6795–6810. https://doi.org/10.1029/2019WR025394

Pfeiffer, A. M., Finnegan, N. J., & Willenbring, J. K. (2017). Sediment supply controls equilibrium channel geometry in gravel rivers. *Proceedings of the National Academy of Sciences*, *114*(13), 3346–3351. https://doi.org/10.1073/pnas.1612907114

Rengers, F. K., McGuire, L. A., Oakley, N. S., Kean, J. W., Staley, D. M., & Tang, H. (2020). Landslides after wildfire: Initiation, magnitude, and mobility. *Landslides*, *17*(11), 2631–2641. https://doi.org/10.1007/s10346-020-01506-3

Roback, K., Clark, M. K., West, A. J., Zekkos, D., Li, G., Gallen, S. F., et al. (2017). The size, distribution, and mobility of landslides caused by the 2015 M_w7.8 Gorkha earthquake, Nepal. *Geomorphology*, *301*, 121–138. https://doi.org/10.1016/j.geomorph.2017.01.030

Rossi, M. W., Whipple, K. X., & Vivoni, E. R. (2016). Precipitation and evapotranspiration controls on daily runoff variability in the contiguous United States and Puerto Rico. *Journal of Geophysical Research: Earth Surface*, *121*(1), 128–145. https://doi.org/10.1002/2015JF003446

Scherler, D., DiBiase, R. A., Fisher, G. B., & Avouac, J.-P. (2017). Testing monsoonal controls on bedrock river incision in the Himalaya and Eastern Tibet with a stochastic-threshold stream power model. *Journal of Geophysical Research: Earth Surface*, *122*(7), 1429. https://doi.org/10.1002/2016JF004011

Seybold, H., Berghuijs, W. R., Prancevic, J. P., & Kirchner, J. W. (2021). Global dominance of tectonics over climate in shaping river longitudinal profiles. *Nature Geoscience*, *14*(7), 7–507. https://doi.org/10.1038/s41561-021-00720-5

Shen, H., Lynch, B., Poulsen, C. J., & Yanites, B. J. (2021). A modeling framework (WRF-Landlab) for simulating orogen-scale climate-erosion coupling. *Computers & Geosciences*, *146*, 104625. https://doi.org/10.1016/j.cageo.2020.104625

Sklar, L. S., & Dietrich, W. E. (2001). Sediment and rock strength controls on river incision into bedrock. *Geology*, *29*(12), 1087–1090. https://doi.org/10.1130/0091-7613(2001)029<1087:SARSCO>2.0.CO;2

Sklar, L. S., & Dietrich, W. E. (2004). A mechanistic model for river incision into bedrock by saltating bed load. *Water Resources Research*, *40*(6), W06301. https://doi.org/10.1029/2003WR002496

Sklar, L. S., & Dietrich, W. E. (2006). The role of sediment in controlling steady-state bedrock channel slope: Implications of the saltation–abrasion incision model. *Geomorphology*, *82*(1–2), 58–83. https://doi.org/10.1016/j.geomorph.2005.08.019

Snyder, N. P., Whipple, K. X., Tucker, G. E., & Merritts, D. J. (2000). Landscape response to tectonic forcing: Digital elevation model analysis of stream profiles in the Mendocino triple junction region, northern California. *Geological Society of America Bulletin*, *112*(8), 1250–1263. https://doi.org/10.1130/0016-7606(2000)112<1250:LRTTFD>2.0.CO;2

Snyder, N. P., Whipple, K. X., Tucker, G. E., & Merritts, D. J. (2003). Importance of a stochastic distribution of floods and erosion thresholds in the bedrock river incision problem. *Journal of Geophysical Research (Solid Earth)*, *108*(B2), 2117. https://doi.org/10.1029/2001jb001655

Sternberg, H. (1875). Untersuchungen über Längen-und Querprofil geschiebeführender Flüsse. *Zeitschrift Für Bauwesen*, *25*, 483–506.

Tucker, G. E. (2004). Drainage basin sensitivity to tectonic and climatic forcing: Implications of a stochastic model for the role of entrainment and erosion thresholds. *Earth Surface Processes and Landforms*, *29*(2), 185–205. https://doi.org/10.1002/esp.1020

Tucker, G. E., & Bras, R. L. (2000). A stochastic approach to modeling the role of rainfall variability in drainage basin evolution. *Water Resources Research*, *36*(7), 1953–1964. https://doi.org/10.1029/2000wr900065

Turowski, J. M., Badoux, A., Leuzinger, J., & Hegglin, R. (2013). Large floods, alluvial overprint, and bedrock erosion. *Earth Surface Processes and Landforms*, *38*(9), 947–958. https://doi.org/10.1002/esp.3341

Webb, R. H., Magirl, C. S., Griffiths, P. G., & Boyer, D. E. (2008). Debris flows and floods in southeastern Arizona from extreme precipitation in July 2006—Magnitude, frequency, and sediment delivery. In *Debris flows and floods in southeastern Arizona from extreme precipitation in July 2006—magnitude, frequency, and sediment delivery (USGS Numbered Series No. 2008–1274; Open-File Report, Volumes 2008–1274)*. U.S. Geological Survey. https://doi.org/10.3133/ofr20081274

Whipple, K. X., Hancock, G. S., & Anderson, R. S. (2000). River incision into bedrock: Mechanics and relative efficacy of plucking, abrasion, and cavitation. *Geological Society of America Bulletin*, *112*(3), 490–503. https://doi.org/10.1130/0016-7606(2000)112<490:riibma>2.0.co;2

Whipple, K. X., & Tucker, G. E. (1999). Dynamics of the stream-power river incision model: Implications for height limits of mountain ranges, landscape response timescales, and research needs. *Journal of Geophysical Research*, *104*(B8), 17661–17674. https://doi.org/10.1029/1999JB900120

Wong, M., & Parker, G. (2006). Reanalysis and correction of bed-load relation of Meyer-Peter and Müller using their own database. *Journal of Hydraulic Engineering*, *132*(11), 1159–1168. https://doi.org/10.1061/(ASCE)0733-9429(2006)132:11(1159)

Yanites, B. J. (2018). The dynamics of channel slope, width, and sediment in actively eroding bedrock river systems. *Journal of Geophysical Research: Earth Surface*, *123*(7), 1504–1527. https://doi.org/10.1029/2017JF004405

Yanites, B. J., Mitchell Nate, A., Bregy Joshua, C., Carlson Grace, A., Kirstyn, C., Margaret, H., et al. (2018). Landslides control the spatial and temporal variation of channel width in southern Taiwan: Implications for landscape evolution and cascading hazards in steep, tectonically active landscapes. *Earth Surface Processes and Landforms*, *43*(9), 1782–1797. https://doi.org/10.1002/esp.4353

Yanites, B. J., & Tucker, G. E. (2010). Controls and limits on bedrock channel geometry. *Journal of Geophysical Research*, *115*(F4), 17. https://doi.org/10.1029/2009JF001601

Yanites, B. J., Tucker, G. E., Hsu, H.-L., Chen, C., Chen, Y.-G., & Mueller, K. J. (2011). The influence of sediment cover variability on long-term river incision rates: An example from the Peikang River, central Taiwan. *Journal of Geophysical Research*, *116*(F3), F03016. https://doi.org/10.1029/2010JF001933